

Social Network Structure Shapes Innovation: Experience-sharing in RL with SAPIENS

Eleni Nisioti¹ Mateo Mahaut^{2 *} Pierre-Yves Oudeyer¹
Ida Momennejad^{3 †} Clément Moulin-Frier^{1 †}

¹ Flowers Team, Inria and Ensta ParisTech, Bordeaux, France

² University Pompeu Fabra, Barcelona, Spain ³ Microsoft Research, New York, US

Abstract

The human cultural repertoire relies on innovation: our ability to continuously and hierarchically explore how existing elements can be combined to create new ones. Innovation is not solitary, it relies on collective accumulation and merging of previous solutions. Machine learning approaches commonly assume that fully connected multi-agent networks are best suited for innovation. However, human laboratory and field studies have shown that hierarchical innovation is more robustly achieved by dynamic communication topologies. In dynamic topologies, humans oscillate between innovating individually or in small clusters, and then sharing outcomes with others. To our knowledge, the role of multi-agent topology on innovation has not been systematically studied in machine learning. It remains unclear a) which communication topologies are optimal for which innovation tasks, and b) which properties of experience sharing improve multi-level innovation. Here we use a multi-level hierarchical problem setting (WordCraft), with three different innovation tasks. We systematically design networks of DQNs sharing experiences from their replay buffers in varying topologies (fully connected, small world, dynamic, ring). Comparing the level of innovation achieved by different experience-sharing topologies across different tasks shows that, first, consistent with human findings, experience sharing within a dynamic topology achieves the highest level of innovation across tasks. Second, experience sharing is not as helpful when there is a single clear path to innovation. Third, two metrics we propose, conformity and diversity of shared experience, can explain the success of different topologies on different tasks. These contributions can advance our understanding of optimal AI-AI, human-human, and human-AI collaborative networks, inspiring future tools for fostering collective innovation in large organizations.

1 Introduction

Collective innovation is a vital manifestation of intelligence. Unlike herds or swarms, human social networks solve different tasks with different communication network topologies (i.e. who communicates with whom) (Momennejad, 2022). Human studies show that while some network topologies (e.g., with high connectivity) are better suited for convergence among networks (Coman et al., 2016; Momennejad et al., 2019), others (e.g., with dynamic and partial connectivity) are best suited for innovation (Derex and Boyd, 2016). However, machine learning approaches to multi-agent learning rarely consider communication topologies that are not fully connected (Mnih et al., 2016; Horgan et al., 2018; Espeholt et al., 2018; Nair et al., 2015; Christianos et al., [n.d.]; Schmitt et al., 2019). Here we test the performance of different multi-agent topologies, in which a group of 10

*Work done during internship at the Flowers Team

†Co-last author

DQNs share their experience to solve diverse tasks of hierarchical innovation. We introduce SAPIENS, an algorithm for Structuring multi-Agent toPology for Innovation through ExperieNce Sharing.

Innovation lies at the core of the human capacity to acquire new skills through open-ended and continual learning and exploration (Leibo et al., 2019). The solitary genius narrative can be misleading: innovation is often a result of recombining and modifying solutions provided by a continuous collective exploration of vast hierarchical search spaces (Solé et al., 2013), e.g., Gutenberg repurposed the screw press to invent the print press. This process is called cumulative cultural evolution (Derex and Boyd, 2016; Mesoudi and Thornton, [n.d.]), in which previous innovations act as a curriculum for future ones. Notably, finding optimal solutions to a task by cumulative culture is highly dependent on the topology of communication networks that share knowledge, with some topologies leading to sub-optimal solutions.

In fact laboratory and field studies of human groups have shown that collective innovation is highly contingent on the social network structure, which dictates who shares experiences with whom (Momennejad, 2022; Migliano and Vinicius, 2022; Derex and Boyd, 2016). This body of human research points to a trade-off: full connectivity (e.g., when everyone talks to everyone) increases the spread and *conformity* of shared knowledge within the group, but simultaneously reduces the *diversity* of solutions (Momennejad et al., 2019). On the other hand, dynamically connected groups oscillate between sparser and denser connectivity, where sparse connectivity periods promote exploration of diverse solutions among group members, while denser connectivity recombines the solutions facilitating the discovery of the global optimum (Derex and Boyd, 2016).

In this paper we propose SAPIENS, an algorithm for Structuring multi-Agent toPology for Innovation through ExperieNce Sharing ³ SAPIENS connects 10 (or more) DQN learners (Mnih et al., 2013) that independently explore the same environment and share their experiences (i.e., experience tuples from their replay buffers) with their neighbors in different topologies.

We employ Wordcraft (Jiang et al., 2020) as a test-bed for evaluating hierarchical innovation in SAPIENS. We design three custom tasks (Figures 1 and 3) covering innovation challenges of different complexity: (i) a task with a single innovation path to an easy-to-find global optimum; (ii) a task with two paths that individually lead to local optima, but when combined, can merge toward the global optimum; (iii) a task with 10 paths, only one of which leads to the global optimum (that is hard to find due to a vast search space).

Inspired by human studies, we compare the performance of SAPIENS with different topologies on the three innovation tasks described above. We empirically show that the relative performance of SAPIENS groups depends on the inter-play between their communication network topology and task demands. In particular, the dynamic structure performs most robustly, exhibiting an impressive ability to converge quickly in the easy task, avoid local optima in the second task, and explore efficiently in the third task. We propose and compute measures of conformity and diversity (Momennejad et al., 2019) to interpret and discuss these findings

2 Methods

2.1 Wordcraft: a test-bed for innovation

We perform experiments on Wordcraft (Jiang et al., 2020), an environment inspired from the game Little Alchemy 2 ⁴ In Wordcraft, one starts with an initial set of elements and explores combinations of two elements in order to create new ones. Elements never disappear, which leads to a progressive increase in the number of available elements with crafting time. Figure 1 (Left) provides an illustrative example.

In Wordcraft one can create different types of tasks using a *recipe book* (\mathcal{X}_{valid}), which is a dictionary containing the valid element combinations with entries in the form $(x, y) \rightarrow z$, where x and y indicate the two chosen elements and z the newly crafted one. When queried with a non-valid combination \mathcal{X}_{valid} returns no element. In addition to the recipe book, a task requires a reward function R_{valid} that returns a scalar reward associated with crafting element z . A valid combination returns a new

³We provide an implementation of SAPIENS and code to reproduce all results reported in this paper in <https://github.com/eleninisioti/SAPIENS>.

⁴<https://littlealchemy2.com/>.

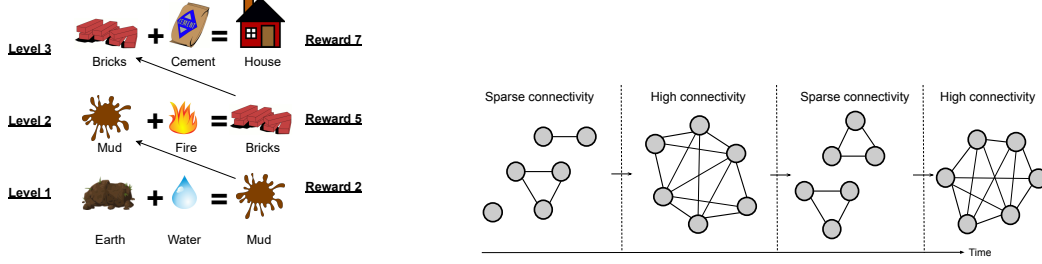


Figure 1: (Left) Illustration of an innovation task: the task consists of an initial set of elements (Earth, Water) and a recipe book that determines which element combinations create new elements. Some elements, such as Earth + Mud, cannot be combined. Upon creating a new element the player moves one innovation level higher and receives a reward that increases monotonically with levels (Right) Dynamic social network structures oscillate between phases of low connectivity, where experience sharing takes place within clusters, and high connectivity, where experiences spread between clusters

element and reward only the first time it is chosen. When queried with a non-valid combination, \mathcal{R}_{valid} returns a reward of zero. Thus, a task can be described by a tuple $(\mathcal{X}_0, \mathcal{X}_{valid}, \mathcal{R}_{valid}, T)$, where \mathcal{X}_0 denotes the initial set of elements and T is the number of time steps available to an agent before the environment resets. The environment can therefore be modeled as a fully-observable Markov Decision Process (MDP) that we define in detail in Appendix 7.1.

2.2 Innovation tasks

We design three recipe books that are shown in Figure 2 and differ in the optimization challenge they pose to RL agents:

Single innovation path The recipe book consists of an initial set of 3 base elements ($\mathcal{X}_{valid} = \{a_1, a_2, a_3\}$) and 8 innovation levels. To create the first element an agent needs to combine two of them. To progress further the agent needs to combine the most recently created element with an appropriate one from the initial set. This optimization problem contains a single global optimum.

Merging paths There are two independent paths, A and B, and at level 2 there is a cross-road that presents the player with three options: moving forward on path A, moving forward on path B, or combining elements from path A and B to progress on path C. The latter path is more rewarding and is, thus, the optimal choice. This path is particularly challenging: to explore path C the player needs to first go to lower innovation levels instead of just progressing on a single path. This task thus exhibits two local optimum (8 elements on A, 8 elements on B) and one global optimum (2 elements on path A + 2 elements on path B + 4 elements on path C).

Best-of-ten paths Here, there are ten paths one of which is the most rewarding. The optimal strategy is to move only on the most rewarding path but, to do so, the player must first explore and reject the other paths. This optimization task is characterized by a single global optimum and aims at evaluating the ability of agents to explore effectively in large spaces.

We make use of the following concepts to characterize the structure of innovation tasks. First, we note that an innovation task can contain one or more paths and that paths can potentially be connected to each other (as in the merging paths task). In our proposed tasks, an **innovation path** X is defined as a sequence of elements $[x_1, \dots, x_n]$, where crafting an element x_i ($i > 1$) requires to combine the previously crafted element x_{i-1} and a base element from the initial set. The first element x_1 in the sequence requires combining elements from the initial set or from other paths. The **innovation level** of an element corresponds to the length of the path it belongs to, plus the sum of the path lengths required to craft its first item (0 if the first item is crafted from base elements). For example, the innovation level of A_3 in the single path task is 3, while the innovation level of element C_1 in the merging paths task is 5 (1 on C + 2 on A + 2 on B). Within an innovation task, the **trajectory** of an agent defined as the sequence of crafted elements it produces. Finally, the **optimal trajectory** of an innovation task is the trajectory that returns the highest cumulative reward within the problem horizon T . In all our tasks, the reward returned by elements in the same innovation path increases

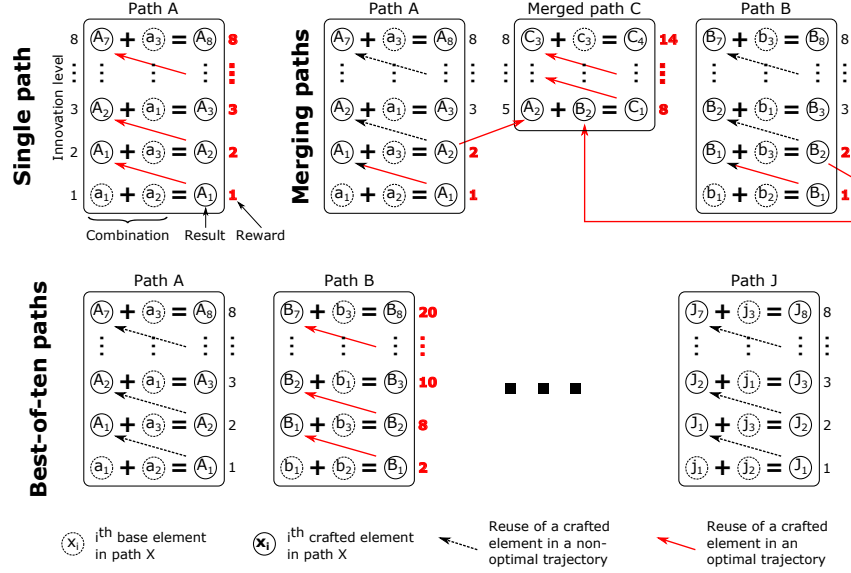


Figure 2: We evaluate our algorithm on three innovation tasks called single path, merging paths and best-of-ten paths, which are explained in section 2.2. Each task contains one or more paths, labeled by an uppercase letter (A to J). Each path X has its own initial set of three base elements $\{x_1, x_2, x_3\}$, which are represented in dashed circles. Crafted elements in path X are represented in upper case (X_i) in solid circles. Optimal trajectories for each tasks are represented by solid red arrows, with their corresponding reward in bold red.

monotonically with the level. However, some paths may be more rewarding than others so that two elements may return different rewards even if they have the same innovation level (see Figure 2).

2.3 Learning algorithm

SAPIENS considers a group of K DQN agents, where each agent interacts with its own copy of the environment. An agent can share experiences with another agent by randomly sampling transition tuples from its own replay buffer and directly inserting them to the replay buffer of the other agent. A graph \mathcal{G} determines who shares information with whom. \mathcal{G} is a set of nodes, representing agents, and edges indicating that two agents share experiences with each other. We define the neighborhood of agent k as the set of nodes connected to it and denote it as \mathcal{N}_k . At the end of each episode the agent shares experiences with each of its neighbors with probability p_s : sharing consists of sampling a random subset of experiences of length L_s from its own buffer B_k and inserting it in the buffers of all neighbors $B_n, n \in \mathcal{N}_k$. Thus, an agent communicates distinct experiences with each of its neighbors. We present a schematic of two DQN agents sharing experiences on the right of Figure 3 and the pseudocode of our learning algorithm in Appendix 7.3. We also provide more implementation details about the DQN in Appendix 7.1.

On the left of Figure 3 we visualize the communication network topologies studied in our work: fully-connected, small-world, ring and dynamic. We construct the latter topology by grouping the agents in pairs and then allowing agents to visit other groups for a specified duration with a certain probability. We provide more information about the implementation of the small-world and dynamic topologies in Appendix 7.2.

2.4 Evaluation framework

During evaluation trials, which take place every E_{eval} training steps with exploration and experience sharing deactivated, we compute the following metrics (indexed by the training step t at which they were computed):

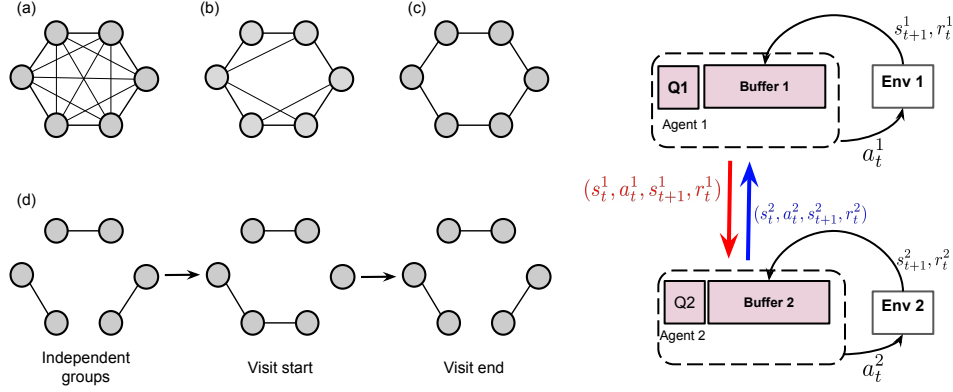


Figure 3: (Left) Visualizing communication graphs (a) fully-connected (b) small-world (c) ring (d) dynamic. (Right) Schematic of two neighboring DQNs sharing experiences: agent 1 shares experiences from its own replay buffer to that of agent 2 (red arrow) and vice versa (blue arrow) while both agents are independently collecting experiences by interacting with their own copy of the environment.

Performance-based metrics This family of metrics describes the quality of the final solution and the speed of convergence to it. Specifically: (i) R_t^+ : the maximum reward of the group at training step t ; (ii) R_t^* : the average reward of the group at training step t ; (iii) T^+ , Time to first success: the first training step at which at least one of the agents collected the maximum achievable reward; (iv) T^* , Time to all successes: the first training step at which all of the agents found the optimal solution (v) $T^>$, Spread time: number of training steps required for the optimal solution to spread to the whole group, once at least one member discovered it (equals $T^* - T^+$) (vi) S^G , % of group success, denotes the percentage of trials in which at least one agent in a group found the optimal solution

Behavioral metrics This family of metrics characterizes the policies followed by the agents. Specifically: (i) conformity C_t is a group-level metric that denotes the percentage of agents in a group that followed the same trajectory in a give evaluation trial (ii) volatility V_t is an agent-level metric that denotes the cumulative number of changes in the trajectory followed by an agent.

Mnemonic metrics These metrics aim to characterize the replay buffer of agents. In particular: (i) diversity D_t^k is an agent-level metric that denotes the number of unique experiences in the replay buffer of an agent; (ii) D_t^G is a group-level metric that captures the diversity of the aggregated group buffer. To compute it we concatenate the replay buffers of all agents into a single one and compute its diversity;.

3 Results

We now evaluate the social network structures presented in Figure 3 on the innovation tasks described in Section 2.2 and visualized in Figure 2. We also compare with a setting without experience sharing that we refer to as *no-sharing*. We employ groups of 10 DQNs with the same hyperparameters across tasks (see Appendix for hyperparameter values 7.4.1. We also perform a study of how results scale for different group sizes ($K = 2, 6, 10, 20, 50$ that we report in Appendix 7.4.4. We perform 20 independent trials and present 95% confidence intervals. In the dynamic topology the probability of visiting another group is 0.01 and the visit lasts for 10 consecutive episodes. (We provide results for different implementations of the dynamic structure in Appendix 7.4.5)

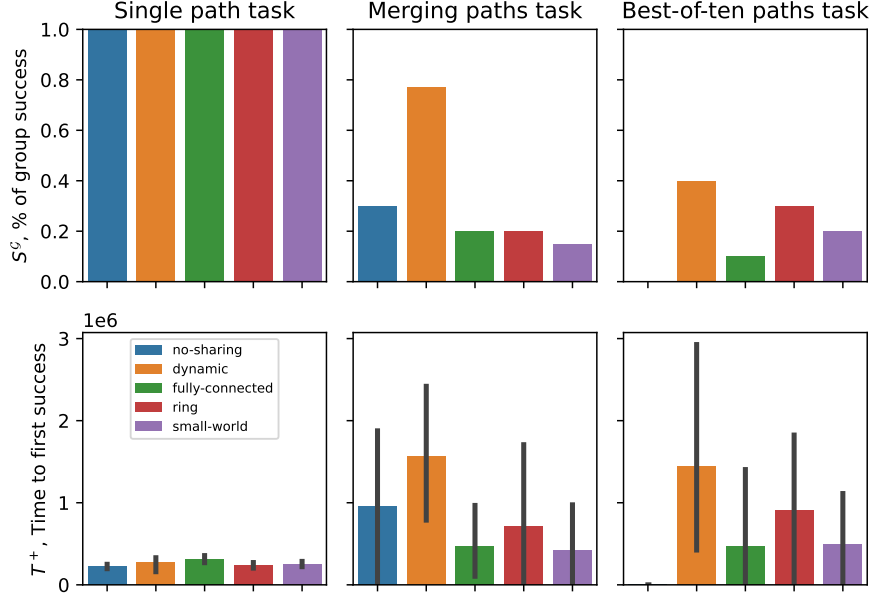


Figure 4: Overall comparison of performances for the single path task (first column), merging paths task (second column) and best-of-ten paths task (third column). We present two metrics: S^G %, of group success denotes the percentage of trials in which at least one agent in the group found the optimal solution (top row) and T^+ , Time to first success, which is the number of training time steps required (second for group success (bottom row)

3.1 Overall comparison

In Figure 4 we compare performance across tasks and structure, in particular (S^G %, of group success) in the first row and the convergence rate of the group to the optimal solution (T^+ , Time to first success) in the second row. We observe that performance varies across tasks and structures: the single path task is optimally solved by all settings with the fully-connected group being the slowest to converge, this difference being statistically significant. The merging paths task is most successfully solved by the dynamic setting (80%), which was also slower than others. In the best-of-10 paths task, the communication networks with lower connectivity (dynamic, ring and small-world) have the highest probability of succeeding.

We now study each task in isolation focusing on the behavioral and mnemonic metrics described in Section 2.4 to explain the observed differences. We visualize the conformity (C_t) and average diversity (D_t) for the single path task in Figure 5 and the volatility (V_T) and group diversity (D_t^G) for all three tasks in Figure 6. We also refer the reader to Appendix for more tables and figures.

For each task, we focus on the conformity and volatility behavioral metrics and, when necessary, refer the reader to more results in Appendix 7.4.

3.2 Task: Single path

The main qualitative conclusion in this task is that although all topologies found the optimal solution, experience sharing does not improve performance (see Appendix 7.4.2 for values of all performance-based metrics). It even slows down learning when connectivity is high (fully-connected group).

While it is not surprising that a single agent with random exploration can efficiently solve a task with a single global optimum, it is not clear at first glance why experience sharing harms performance. Notably this phenomenon has been observed in related works (Souza et al., 2019; Schmitt et al., 2019). We also observed that, when we look at aT^* the fully-connected group was quicker than the dynamic and no-sharing settings. This can be explained by looking at conformity C_t on the left of Figure 5: fully-connected exhibits higher conformity than the dynamic and no-sharing setting. Thus,

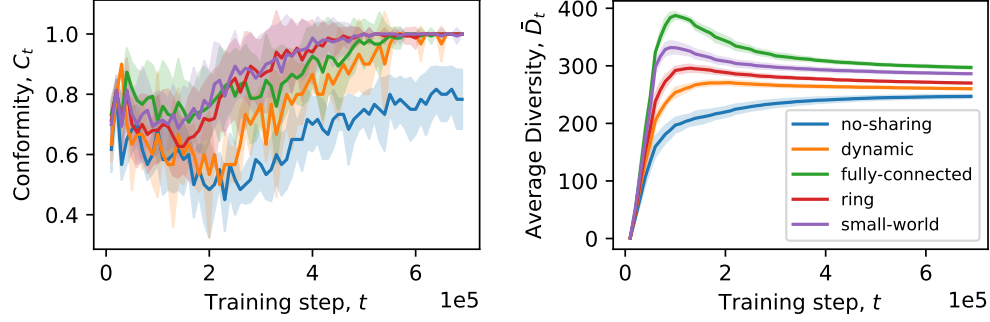


Figure 5: Analyzing group behavior in the single path task:: (left) Conformity C_t is a behavioral metric that denotes the percentage of agents in a group that followed the same trajectory in a given evaluation trial (right) Average Diversity \bar{D}_t is a mnemonic metric that denotes the number of unique experiences in the replay buffer of an agent, averaged over all agents

information sharing ensures that once at least one agent has found the optimal solution, this spreads to the whole group. This is most prevalent in the small-world topology which has a statistically significant smaller value ($T^> = 49333$) compared to all other topologies. Perhaps surprisingly, the fully-connected group does not have the highest conformity. We therefore conclude that there is an upper threshold for connectivity, beyond which shared experiences destabilize learning. We can detect this destabilization when looking at volatility V_t , which is highest for the fully-connected setting (top left plot in Figure 6). We believe that this instability is caused by the diversity in the replay buffer of each agent, captured by the average individual diversity metric \bar{D}_t (right in Figure 5): agents in the fully-connected network have the most diverse buffers while agents in the no-sharing setting have the least diverse buffers. As DQNs sample their replay buffer randomly and the task is simple, low diversity of individual buffers leads to quicker convergence.

Finally, when looking at the group diversity in Figure 6, fully-connected ranks last and the dynamic topology ranks first. This is rather surprising: the no-sharing setting does not rank first, but experience sharing increases the diversity of a group when connectivity is low, and, most prevalently, when the topology is dynamic. This indicates that shared experiences foster exploration.

3.3 Task: Merging paths

In this task we observed that the dynamic topology succeeded with the highest probability but took longer compared to other structures. We hypothesize that these observations are inter-connected: avoiding the two local optima in this task requires prolonging exploration after the local optimum has been found. Thus, by converging more slowly the dynamic network increases its chances of finding the optimal solution. Instead, the other structures either find the global optimum quickly (if an agent discovers it by chance before being drawn to the local optimum by others) or miss it entirely. We can see this maintenance of exploration in the lower conformity of the dynamic structure (C_t remains around 0.6 for the dynamic, around 0.4 for the no-sharing setting and around 0.8 for the other multi-agent topologies). The ring topology, the static structure with the lowest connectivity, exhibits a similar behavior to the dynamic structure.

Finally, when doing an overall comparison with the previous task, we observe that the behavioral and mnemonic metrics vary quantitatively but the qualitative difference is not significant: the different social network structures rank in the same order for the two tasks. The only notable difference is that diversity, both for individual agents and the group, persists longer in this task, due to the fact that the optimal solution has not been found yet.

3.4 Task: Best-of-ten path

In this task we observed that groups with lower connectivity explore more efficiently. The dynamic topology had the highest group success rate ($S_t^G = 0.4$), the no-sharing setting failed to reach beyond the second level of the optimum path ($R_t^+ = 0.2$) and continued exploring the other paths, while the

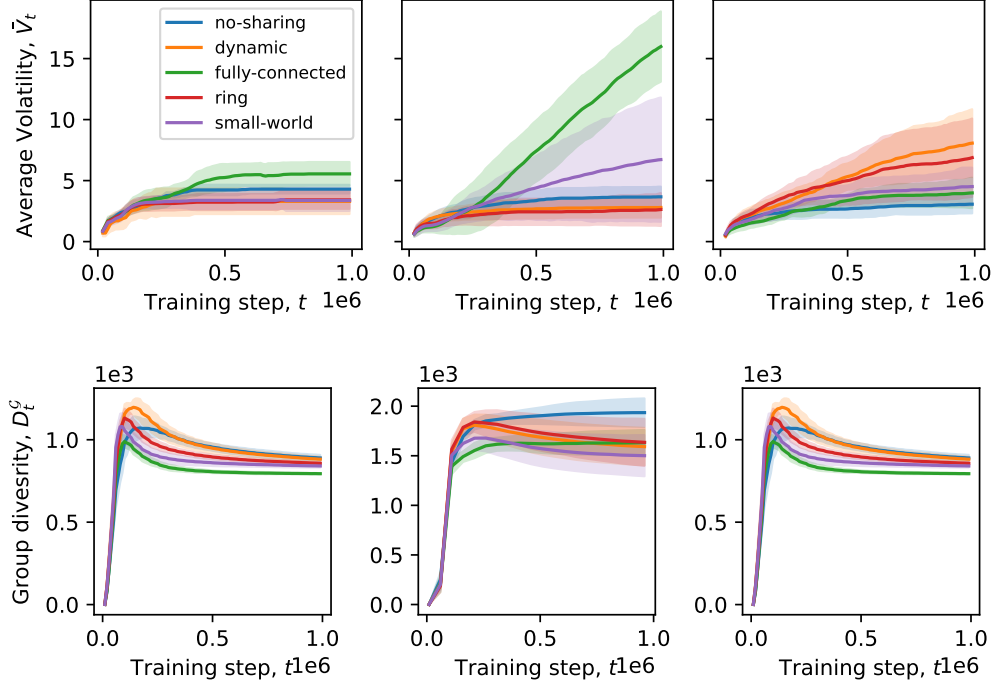


Figure 6: Analyzing group behavior in the single path task (first column), merging paths task (second column) and best-of-10 paths task (third column). On the top row, the Average volatility (V_t) is a behavioral metric indicating the cumulative number of changes in the trajectory followed by an agent, averaged by all agents. On the bottom row, Group Diversity D_t^G is a mnemonic metric that captures the diversity of the aggregated group buffer.

fully-connected groups discovered the optimal path but did not progress far on it ($(R_t^+ = 0.4)$). (We provide detailed results about the trajectories followed by different agents in this task in Appendix 7.4.2)

Observing the metrics in Figure 6 we see that this task differs significantly from the previous two: 1. volatility (V_t top right in Figure 6) is highest for the dynamic and ring topologies. As these are the topologies with the highest success rate, we conclude that low connectivity is crucial for exploration of large spaces, as it ensures that the group does not converge prematurely; 2. in the no-sharing setting, group diversity (D_t^G bottom right) is lowest. This comes in stark contrast to the two previous tasks, where this setting exhibited high diversity. Thus, similarly to the dynamic setting in the single path task, experience sharing fosters exploration

4 Related work

The hypothesis that the structure of communication networks affects the innovation abilities of groups has been studied in human psychology and ecology (Mason et al., 2008; Derex and Boyd, 2016; Mason and Watts, 2012). The literature points to the interplay of communication network topology and task structure, with tasks exhibiting local minima being solved better by partially connected groups. Properties of certain structures such as information propagation (Watts and Strogatz, 1998) and mobility (Sicardi et al., 2009) have been linked to the learning benefits of information sharing. With this work we propose that DRL can be a powerful computational tool for evaluating such studies on more complex tasks.

Experience sharing among RL agents solving a task can significantly improve both convergence rate and performance (Horgan et al., 2018; Mnih et al., 2016; Schmitt et al., 2019; Nair et al., 2015). It may involve sharing experience tuples or sharing gradients. The former is common among off-policy algorithms (Souza et al., 2019; Horgan et al., 2018; Mnih et al., 2016) and bares benefits over sharing

gradients in actor-critic architectures, where instability and latency are concerns (Schmitt et al., 2019; Christianos et al., [n.d.]).

A common architecture for experience sharing is that of multiple actors collecting experience in a single replay buffer, on which a single learner is trained (Mnih et al., 2016; Horgan et al., 2018; Schmitt et al., 2019). For instance, the Gorila framework (Nair et al., 2015), introduced a generic, customizable multi-learner architecture with both local and global replay buffers, but focused on parameter sharing rather than experience sharing. Another approach included experience sharing between actors but the groups only included two agents, that requested experiences instead of transmitting them (Souza et al., 2019). Moreover, a simple agent-based model solving line search compared the performance of different topologies but not dynamic typologies and not for innovation tasks (Lazer and Friedman, 2007).

Our approach is different from previous work in three ways. First, we focus on tasks that require multi-level hierarchical innovation. Second, our deep RL agents explore solutions in parallel while sharing experiences. Third, SAPIENS structures agents in different topologies of experience sharing to investigate the interplay of multi-agent topology and task structure that together shape performance.

5 Discussion and Future Work

From tool use and language to music and mathematics, human innovation is shaped by cumulative solutions, combining knowledge developed across social networks. Human studies have shown that different topologies of communication networks are best suited to solve different tasks. However, most machine learning approaches to multi-agent RL assume static, often fully-connected networks. Here we test the hypothesis that the topology of experience sharing in a network of multiple deep RL agents can shape the network’s cumulative innovation. We have proposed SAPIENS, a flexible multi-agent algorithm Structuring multi-Agent topology for Innovation through ExperieNce Sharing. SAPIENS experiments show that dynamic topologies of experience sharing are best suited to solve complex multi-level innovation tasks.

Our empirical results show that both social network topology and task structure affect the performance of SAPIENS. We find that, first, consistent with human findings, experience sharing within a dynamic topology achieves the highest level of innovation across tasks. Second, experience sharing is not as helpful when there is a single clear path to innovation. We propose metrics of diversity and conformity to explain the success and failure modes of experience sharing topologies.

Recent multi-agent studies have used experience sharing in parallel learning and have empirically demonstrated both successes and failures. Some suggest simple benefits in computation time that allow scaling up existing implementation of off-policy learners (Nair et al., 2015), while others report surprising benefits not just in convergence time but also in the quality of the final solution (Horgan et al., 2018; Christianos et al., [n.d.]). The latter is attributed to improved exploration due to the diversity of experiences collected by agents who differ in their hyper-parameterization (e.g. exploration schedule or discount factor). However, no work has explicitly measured the diversity of experiences to test this hypothesis. Moreover, the failure modes of multi-agent approaches in some Atari (Schmitt et al., 2019) and control games (Souza et al., 2019) are not well understood. In our work we propose behavioral and mnemonic metrics and show that they can help explain the observed differences in behaviors. We demonstrate that, even if the agents in a group are identical, diversity and performance vary with *communication topology*. Thus, we suggest that the structure of communication networks is a parameter orthogonal to individual diversity.

We believe that scaling up our study by applying SAPIENS in environments commonly employed by the multi-agent reinforcement learning community to study innovation (Leibo et al., 2019), that for example include tasks such as foraging and crafting is an important next step.

Note that while the present implementation considers groups of DQN agents, SAPIENS is agnostic to the choice of off-policy algorithm. In future studies we plan to investigate SAPIENS networks with different types of RL agents, and further analyze the interplay of topology, task, learner-type. For instance, we could identify what network role (e.g. centrality, brokering, bridging, etc) is best suited for which learning agents across different tasks. We also envision a meta-learning version of SAPIENS where an outer-loop optimizes the social network structure.

Such future studies can have wide societal implications, paving the way toward predicting optimal structures of communication for human-AI cooperation networks, and simulating optimal human-human topologies for innovation, e.g. in large organization. In an era of pending climate catastrophes and global pandemics, designing optimal collaboration networks could enhance the survival of our species. We believe SAPIENS can shed light on how to optimize communication topologies to solve a wide range of innovation tasks in diverse and scaled AI-AI, human-AI, and human-human networks, and lead to future tools for fostering human and machine innovation in large organizations.

6 Acknowledgments

This research was partially funded by the the Inria Exploratory action ORIGINS (<https://www.inria.fr/en/origins-grounding-artificial-intelligence-origins-human-behaviour>) as well as the French National Research Agency (<https://anr.fr/>, project ECOCURL, Grant ANR-20-CE23-0006). This work also benefited from access to the HPC resources of IDRIS under the allocation 2020-[A0091011996] made by GENCI, using the Jean Zay supercomputer.

References

- Filippos Christianos, Lukas Schäfer, and Stefano V Albrecht. [n.d.]. Shared Experience Actor-Critic for Multi-Agent Reinforcement Learning. ([n. d.]), 11.
- Alin Coman, Ida Momennejad, Rae D Drach, and Andra Geana. 2016. Mnemonic convergence in social networks: The emergent properties of cognition at a collective level. *Proc. Natl. Acad. Sci. U. S. A.* 113, 29 (July 2016), 8171–8176.
- Maxime Derex and Robert Boyd. 2016. Partial connectivity increases cultural accumulation within groups. *Proceedings of the National Academy of Sciences* 113, 11 (March 2016), 2982–2987. <https://doi.org/10.1073/pnas.1518798113>
- Robin I. M. Dunbar. 2014. How conversations around campfires came to be. *Proceedings of the National Academy of Sciences* 111, 39 (Sept. 2014), 14013. <https://doi.org/10.1073/pnas.1416382111>
- Lasse Espeholt, Hubert Soyer, Remi Munos, Karen Simonyan, Volodymir Mnih, Tom Ward, Yotam Doron, Vlad Firoiu, Tim Harley, Iain Dunning, Shane Legg, and Koray Kavukcuoglu. 2018. *IMPALA: Scalable Distributed Deep-RL with Importance Weighted Actor-Learner Architectures*. Technical Report arXiv:1802.01561. arXiv. <http://arxiv.org/abs/1802.01561> arXiv:1802.01561 [cs].
- Dan Horgan, John Quan, David Budden, Gabriel Barth-Maron, Matteo Hessel, Hado van Hasselt, and David Silver. 2018. Distributed Prioritized Experience Replay. *arXiv:1803.00933 [cs]* (March 2018). <http://arxiv.org/abs/1803.00933> arXiv: 1803.00933.
- Minqi Jiang, Jelena Luketina, Nantas Nardelli, Pasquale Minervini, Philip H. S. Torr, Shimon Whiteson, and Tim Rocktäschel. 2020. WordCraft: An Environment for Benchmarking Commonsense Agents. *arXiv:2007.09185 [cs]* (July 2020). <http://arxiv.org/abs/2007.09185> arXiv: 2007.09185.
- Diederik P. Kingma and Jimmy Ba. 2014. Adam: A Method for Stochastic Optimization. <http://arxiv.org/abs/1412.6980> cite arxiv:1412.6980Comment: Published as a conference paper at the 3rd International Conference for Learning Representations, San Diego, 2015.
- Michelle A. Kline and Robert Boyd. 2010. Population size predicts technological complexity in Oceania. *Proceedings of the Royal Society B: Biological Sciences* 277, 1693 (Aug. 2010), 2559–2564. <https://doi.org/10.1098/rspb.2010.0452>
- David Lazer and Allan Friedman. 2007. The Network Structure of Exploration and Exploitation. *Administrative Science Quarterly* 52, 4 (Dec. 2007), 667–694. <https://doi.org/10.2189/asqu.52.4.667>

- Joel Z Leibo, Edward Hughes, Marc Lanctot, and Thore Graepel. 2019. Autocurricula and the emergence of innovation from social interaction: A manifesto for multi-agent intelligence research. *arXiv preprint arXiv:1903.00742* (2019).
- W. Mason and D. J. Watts. 2012. Collaborative learning in networks. *Proceedings of the National Academy of Sciences* 109, 3 (Jan. 2012), 764–769. <https://doi.org/10.1073/pnas.1110069108>
- Winter A. Mason, Andy Jones, and Robert L. Goldstone. 2008. Propagation of innovations in networked groups. *Journal of Experimental Psychology: General* 137, 3 (2008), 422–433. <https://doi.org/10.1037/a0012798>
- Alex Mesoudi and Alex Thornton. [n.d.]. What is cumulative cultural evolution? *Proceedings of the Royal Society B: Biological Sciences* 285, 1880 ([n.d.]), 20180712. <https://doi.org/10.1098/rspb.2018.0712> Publisher: Royal Society.
- Andrea Bamberg Migliano and Lucio Vinicius. 2022. The origins of human cumulative culture: from the foraging niche to collective intelligence. *Philosophical Transactions of the Royal Society B: Biological Sciences* 377, 1843 (Jan. 2022), 20200317. <https://doi.org/10.1098/rstb.2020.0317> Publisher: Royal Society.
- Volodymyr Mnih, Adrià Puigdomènech Badia, Mehdi Mirza, Alex Graves, Timothy P. Lillicrap, Tim Harley, David Silver, and Koray Kavukcuoglu. 2016. Asynchronous Methods for Deep Reinforcement Learning. *arXiv:1602.01783 [cs]* (June 2016). <http://arxiv.org/abs/1602.01783> arXiv: 1602.01783.
- Volodymyr Mnih, Koray Kavukcuoglu, David Silver, Alex Graves, Ioannis Antonoglou, Daan Wierstra, and Martin A. Riedmiller. 2013. Playing Atari with Deep Reinforcement Learning. *CoRR* abs/1312.5602 (2013). arXiv:1312.5602 <http://arxiv.org/abs/1312.5602>
- Ida Momennejad. 2022. Collective minds: social network topology shapes collective cognition. *Philosophical Transactions of the Royal Society B: Biological Sciences* 377, 1843 (Jan. 2022), 20200315. <https://doi.org/10.1098/rstb.2020.0315> Publisher: Royal Society.
- Ida Momennejad, Ajua Duker, and Alin Coman. 2019. Bridge ties bind collective memories. *Nat. Commun.* 10, 1 (April 2019), 1578.
- Arun Nair, Praveen Srinivasan, Sam Blackwell, Cagdas Alcicek, Rory Fearon, Alessandro De Maria, Vedavyas Panneershelvam, Mustafa Suleyman, Charles Beattie, Stig Petersen, Shane Legg, Volodymyr Mnih, Koray Kavukcuoglu, and David Silver. 2015. *Massively Parallel Methods for Deep Reinforcement Learning*. Technical Report arXiv:1507.04296. arXiv. <http://arxiv.org/abs/1507.04296> arXiv:1507.04296 [cs].
- Simon Schmitt, Matteo Hessel, and Karen Simonyan. 2019. *Off-Policy Actor-Critic with Shared Experience Replay*. Technical Report arXiv:1909.11583. arXiv. <http://arxiv.org/abs/1909.11583> arXiv:1909.11583 [cs, stat].
- Estrella A. Sicardi, Hugo Fort, Mendeli H. Vainstein, and Jeferson J. Arenzon. 2009. Random mobility and spatial structure often enhance cooperation. *Journal of Theoretical Biology* 256, 2 (Jan. 2009), 240–246. <https://doi.org/10.1016/j.jtbi.2008.09.022>
- Ricard V. Solé, Sergi Valverde, Marti Rosas Casals, Stuart A. Kauffman, Doyne Farmer, and Niles Eldredge. 2013. The evolutionary ecology of technological innovations. *Complexity* 18, 4 (March 2013), 15–27. <https://doi.org/10.1002/cplx.21436>
- Lucas Oliveira Souza, Gabriel de Oliveira Ramos, and Celia Ghedini Ralha. 2019. Experience Sharing Between Cooperative Reinforcement Learning Agents. *arXiv:1911.02191 [cs]* (Nov. 2019). <http://arxiv.org/abs/1911.02191> arXiv: 1911.02191.
- Duncan J Watts and Steven H Strogatz. 1998. Collective dynamics of ‘small-world’ networks. 393 (1998), 3.
- Polly W. Wiessner. 2014. Embers of society: Firelight talk among the Ju/’hoansi Bushmen. *Proceedings of the National Academy of Sciences* 111, 39 (Sept. 2014), 14027. <https://doi.org/10.1073/pnas.1404212111>

7 Supplementary material

This supplementary material provides additional methods, results and discussion, as well as implementation details.

- Section 7.1 describes in detail the MDP formulation of Wordcraft.
- Section 7.2 explains how we designed small-worlds and two types of dynamic topologies.
- Section 7.3 contains the pseudocode of SAPIENS.
- Section 7.4 provides more information about our experimental setup (DQN hyperparameters) and results (effect of group size, different implementations of dynamic topologies). We also provide tables and figures for all metrics presented in Section 2.4 and introduce two new metrics: intra-group and inter-group alignment.

7.1 Details of Wordcraft as a Markov Decision Process

We consider the episodic setting, where the environment resets at the end of each episode and an agent is trained for E_{train} episodes. At each time step t , the agent observes the state s_t and selects an action a_t from a set of possible actions \mathcal{A} according to its policy π^θ , where π is a mapping from states to actions, parameterized by a neural network with weights θ . In return, the agent receives the next state s_{t+1} and a scalar reward r_t . Each DQN agent collects experience tuples of the form $[s_t, a_t, s_{t+1}, r_t]$ in its replay buffer.

In order to solve an innovation task described in Section 2.1 we compute the maximum number of elements a player can craft within horizon T for recipe book \mathcal{X}_{valid} and initial set \mathcal{X}_0 , which we denote as $|X|$. We, then, encode each element as an integer in $[0, |X|)$. Thus, the action space is $\mathcal{A} = [0, |X|)$, with action a_t indicating the index of the currently chosen element. The state s_t contains two sets of information: a binary vector of length $|X|$ with non-zero entries for elements already crafted by the agent within the current episode (we refer to this as inventory i) and another binary vector of length $|X|$ where an index is non-zero if it is currently selected by the agent (we refer to this as current c). An agent begins with an inventory having non-zero element only for the initial set \mathcal{X}_0 and an all-zero selection. With the first action a_0 , the selected item becomes non-zero in the selection. With the second action, a_1 , we check if the combination (a_1, c_0) is valid under the recipe book and, if so, return the newly crafted element (corresponding entry in i becomes non-zero) and the reward. This two-step procedure continues until the end of the episode. Figure 7 offers a visualization of the states and actions encountered during an episode in Wordcraft, where the chosen actions and elements are chosen so as to reproduce the example of Figure 1.

7.2 Implementation details of social network topologies

7.2.1 Small-world topology

We construct small-worlds using the Watts–Strogatz model (`watts_strogatz_graph` method of the `networkx` package ⁵). This model first builds a ring lattice where each node has n neighbors and then rewires an edge with probability β . Compared to other techniques used in previous works studying the effect of topology Mason et al. (2008), this way of constructing small-worlds ensures that the average path lengths is short and clustering is high. These two properties are what differentiates small-worlds from random (short average path length and small clustering) and regular (long average path length and high clustering) graphs. We employ $n = 4$ and $\beta = 0.2$ in our experiments, which we empirically found to lead to good values of average path length and clustering.

7.2.2 Dynamic topology

We have tried out two ways of constructing dynamic topologies:

- Inspired by graphs employed in human laboratory studies (Derech and Boyd, 2016), we designed graphs where the macro structure of the graph is constant but agents can randomly change their position. In particular, we divide a group of agents into sub-groups of two

⁵<https://networkx.org/>

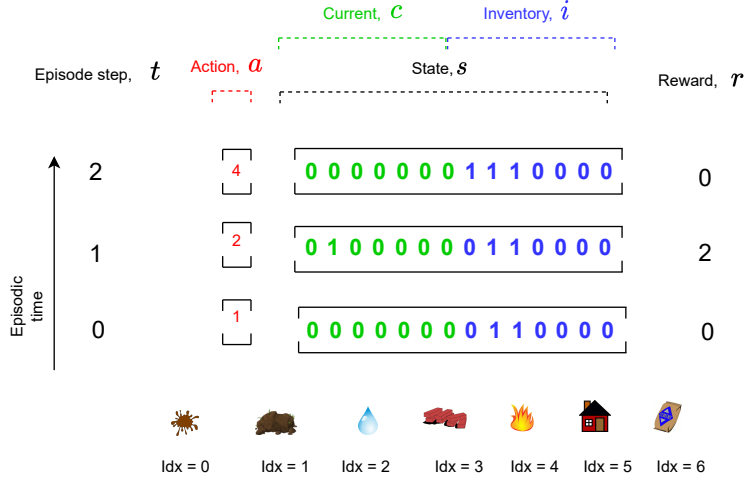


Figure 7: Visualizing actions and states in Wordcraft: we present the first 3 time steps of an episode corresponding to playing the example in Figure 1. This task contains 7 elements, so the action space is an integer with maximum value 7. In the components current c and inventory i , each digit in the vector corresponds to the element with the corresponding index. The initial set includes Water and Earth (their indexes at $\tau = 0$ in the inventory are non-zero). The agent first picks the Earth (second index in the action vector). At $t = 1$, the Earth becomes active in the *Current* vector of the state, the agent selects Water and receives a positive reward. At $t = 2$, Mud is created and inserted in the inventory and c is cleared.

agents and, at the end of each episode, move an agent to another group with a probability p_v for a duration of T_v episodes (for a visualization see Figure 3). To reduce the complexity of the implementation, we assume that only one visit can take place at a time. In the main paper we employ $p_v = 0.01$ and $T_v = 10$ across conditions and present results with different values in Appendix 7.4.5, where we refer to this topology as dynamic-Boyd.

- Human behavioral ecology emphasize the importance of periodic variation in human social networks encountered throughout our evolutionary trajectory Wiessner (2014); Dunbar (2014). Due to ecological constraints human groups oscillate between phases of high and low connectivity: low-connectivity phases arise when individuals need to individually collected resources (e.g. day-time hunting) while high-connectivity phases arise when humans are idle and “forced” to be in proximity with others (e.g. fireside chats). Although these high-connectivity phases do not bare a direct evolutionary advantage, they may have played an important role by creating the conditions for the evolution of human language and culture. Inspired by this hypothesis, we have designed dynamic graphs that oscillate between a fully-connected topology that lasts for T_h episodes and a topology without sharing that lasts for T_l episodes. We present results for various values of T_h and T_l of this topology in Appendix 7.4.5, where we refer to this topology as dynamic-periodic.

7.3 Pseudocode of SAPIENS

We present the pseudocode of our proposed algorithm SAPIENS in Algorithm 1. SAPIENS works similarly to an off-policy reinforcement learning algorithm, with the difference that, after each episode, an experience sharing phase takes place between agents that belong in the same group.

7.4 Empirical results

We presented the major results of our evaluation of SAPIENS in Section 3. We now present additional information regarding the hyper-parameters of the DQN agents (Appendix 7.4.1), the values of all

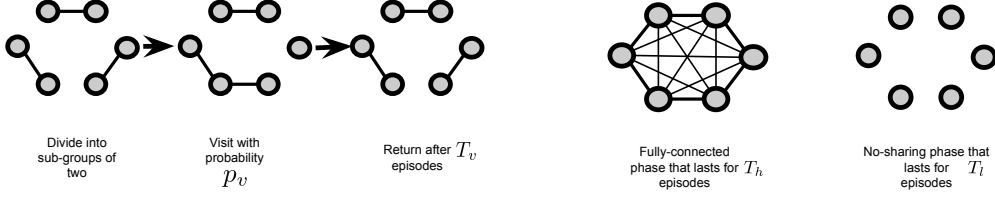


Figure 8: Two types of dynamic topologies: (Left) in the dynamic-Boyd topology the group is divided into sub-groups of two agents and a visit takes place with probability p_v and lasts T_v episodes (Right) In the dynamic-periodic topology the graph oscillates between a phase with a fully-connected topology that lasts for T_h episodes to a phase without sharing that lasts for T_l episodes.

Algorithm 1 SAPIENS (Structuring multi-Agent toPology for Innovation through ExperieNce Shar-ing)

```

1: Input:  $\mathcal{G}, connectivity, R, p_s, LS$ 
2:  $\mathcal{G}.\text{initializeGraph}(connectivity)$ 
3:  $\mathcal{I}.\text{initializeAgent}()$  ▷ Initialize agents
4: for  $i \in \mathcal{I}$  do
5:    $I.\text{neighbors} = I.\text{formNeighborhood}(\mathcal{G})$  ▷ Inform agent about its neighbors
6:    $I.\text{env} = \text{initEnv}(R)$  ▷ Create agent's own copy of the environment based on the recipe book
7: end for
8: while training not done do
9:   for  $i \in \mathcal{I}$  do ▷ Loop through each agent
10:    while episode not done do
11:       $a = i.\text{policy}()$  ▷ Choose action
12:       $r, s_{new} = \text{env}.\text{step}(a)$ 
13:       $i.B.\text{insert}([s, r, a, s_{new}])$ 
14:    end while
15:     $\epsilon = \text{random}()$ 
16:    if  $\epsilon < p_s$  then ▷ Share with probability  $p_s$ 
17:      for  $j \in I.\text{neighbors}$  do
18:         $j.B.\text{add}(i.B.\text{sample}(L))$  ▷ Sample random set of experiences of length  $L$ 
19:      end for
20:    end if
21:     $i.\text{train}()$  ▷ Train agent
22:  end for
23: end while

```

performance metrics and additional plots for experiments discussed in 3 (Appendix 7.4.2), results on intra-group and inter-group alignment (Appendix 7.4.3), results for groups of varying sizes (Appendix 7.4.4) and results on various dynamic topologies (Appendix 7.4.5)

7.4.1 DQN hyperparameters

We employ the same hyper-parameter for each DQN across all studied tasks and topologies: discount factor $\gamma = 0.9$, the Adam optimizer with learning rate $\alpha = 0.001$ (Kingma and Ba, 2014; Dunbar, 2014), ϵ -greedy exploration with $\epsilon = 0.01$. We employ a feedforward network with two layers with 64 neurons each. We implemented SAPIENS by extending the DQN implementation in the stable-baselines3 framework ⁶. For a description of the hyper-parameters of social network topologies and their values we refer the reader to Appendix 7.2

7.4.2 Overall comparison

Tables 1, 2 and 3 contain the values of all metrics discussed in Section 2.4 for the single path, merging paths and best-of-ten paths, respectively. We denote values computed after convergence of the group

⁶<https://stable-baselines3.readthedocs.io/en/master/>

| Topology | R_{∞}^+ | R_{∞}^* | T^+ | T^* | $T^>$ | S^G | C_{avg} | V_{avg} |
|-----------------|----------------|----------------|--------|--------|--------|-------|-----------|-----------|
| no-sharing | 0.9310 | 1 | 228333 | 830000 | 600000 | 1 | 0.7095 | 0.0383 |
| dynamic | 1 | 1 | 270000 | 500000 | 230000 | 1 | 0.8494 | 0.01383 |
| fully-connected | 1 | 1 | 310666 | 362000 | 51333 | 1 | 0.8912 | 0.052 |
| ring | 1 | 1 | 235333 | 305333 | 70000 | 1 | 0.8986 | 0.0280 |
| small-world | 1 | 1 | 253333 | 302666 | 49333 | 1 | 0.912 | 0.02976 |

Table 1: Evaluation metrics for the single path task

| Topology | R_{∞}^+ | R_{∞}^* | T^+ | T^* | $T^>$ | S^G | C_{avg} | V_{avg} |
|-----------------|----------------|----------------|---------|-------|-------|-------|-----------|-----------|
| no sharing | 0.6222 | 0.81 | 3176666 | - | - | 0.3 | 0.4253 | 0.01265 |
| dynamic | 0.7076 | 0.86 | 3124000 | - | - | 0.7 | 0.6444 | 0.0064 |
| fully-connected | 0.5531 | 0.768 | 2370000 | - | - | 0.2 | 0.7456 | 0.1257 |
| ring | 0.6195 | 0.72 | 3540000 | - | - | 0.2 | 0.7779 | 0.012 |
| small-world | 0.5693 | 0.662 | 2800000 | - | - | 0.15 | 0.75772 | 0.0411 |

Table 2: Evaluation metrics for the merging paths task

with underscore ∞ and values averaged over all training steps with underscore avg (note that we use $-$ over variables to denote averaging over agents in a single training step). Cells with a dash (-) indicate that we could not compute the corresponding metrics because a group failed to find a solution in all trials. We also provide the plots of volatility and average diversity for the merging paths and best-of-10 paths task (that were not included in Figure 6) due to page limit constraints).

7.4.3 Measuring inter-group and intra-group alignment

We have so far captures the agreement between agents in a group through the behavioral metric of conformity. Here, we present a mnemonic metric for agreement, which we term alignment. Alignment is a complementary metric to the diversity (D_t^k) and group diversity (D_t^G) metrics, that aims at capturing the effect of experience sharing on the replay buffers in a group. We propose a definition of alignment within a single group (intra-group alignment A_t^G) and a definition of alignment between two different groups ($A_t^{G_j, G_j}$). Such metrics of mnemonic convergence have been linked to social network topology (Coman et al., 2016) and, as we show here, they can prove useful in analyzing groups of reinforcement learning agents.

Specifically: (i) A_t^G is the intra-group alignment. This metric captures the similarity between the replay buffers of agents belonging to the same group. To compute this we compute the size of the disjoint set of experiences for each pair of agents and, then, sum over all these pairs, normalizing in $[0,1]$. (ii) inter-group alignment $A_t^{G_j, G_j}$ is a similar notion of alignment but employed between different groups (e.g. how different is a group of fully-connected and a dynamic group of agents in terms of their group replay buffers?). To compute it we concatenate all replay buffers of a group into a single one and then compute the size of the disjoint set of the two replay buffers.

Figure 10 presents intra-group alignment in the three tasks. **We observe that, in all tasks, intra-group alignment increases with connectivity and that it reduces when the agents enter the exploitation phase. Thus, intra-group alignment can prove useful in characterizing the exploration behavior of a group.** In Figure 11, we present the inter-group alignment in the single path, merging paths and best-of-ten paths tasks. We observe that the topologies do not differ significantly in the single path task. **In the merging task, we observe that inter-group alignment is lower**

| Topology | R_{∞}^+ | R_{∞}^* | T^+ | T^* | $T^>$ | S^G | C_{avg} | V_{avg} |
|-----------------|----------------|----------------|---------|---------|---------|-------|-----------|-----------|
| no sharing | 0.1703 | 0.268 | - | - | - | 0 | 0.37 | 0.009 |
| dynamic | 0.4084 | 0.546 | 4806666 | - | - | 0.4 | 0.41 | 0.03 |
| fully-connected | 0.2183 | 0.238 | 4680000 | 5040000 | 360000 | 0.1 | 0.4784 | 0.0065 |
| ring | 0.4522 | 0.468 | 3010000 | 5030000 | 2440000 | 0.3 | 0.4607 | 0.02308 |
| small-world | 0.2921 | 0.328 | 2455000 | 3970000 | 1515000 | 0.2 | 0.4755 | 0.01418 |

Table 3: Evaluation metrics for the best-of-ten paths task

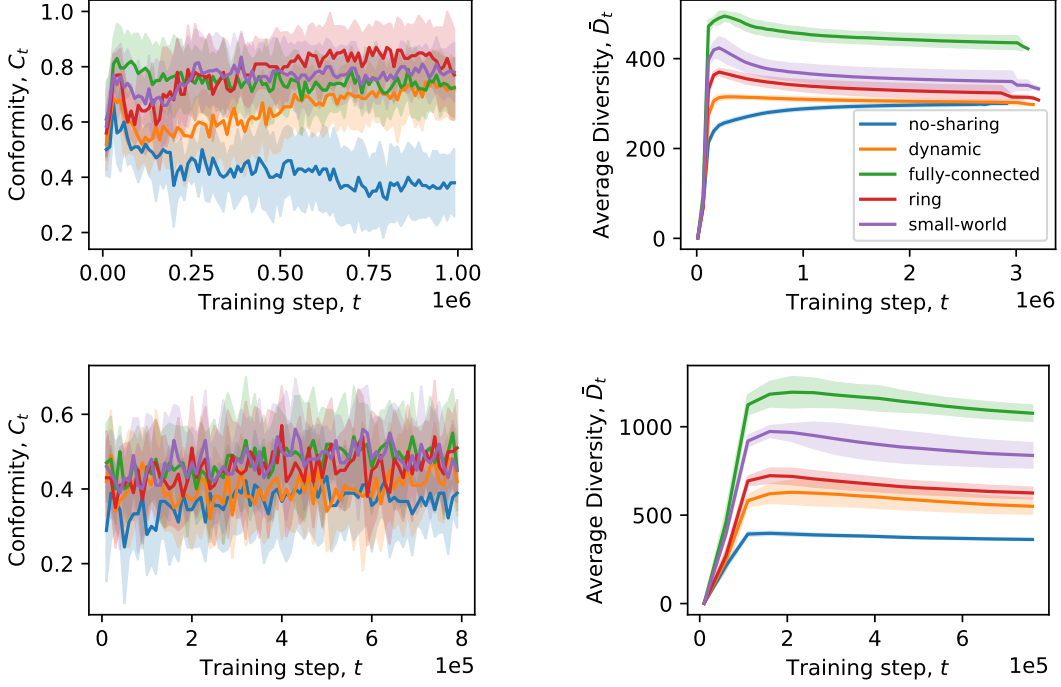


Figure 9: Analyzing group behavior in the merging paths task (top row) and best-of-10 paths task (bottom row). (left) Conformity C_t is a behavioral metric that denotes the percentage of agents in a group that followed the same trajectory in a given evaluation trial (right) Average Diversity \bar{D}_t is a mnemonic metric that denotes the number of unique experiences in the replay buffer of an agent, averaged over all agents.

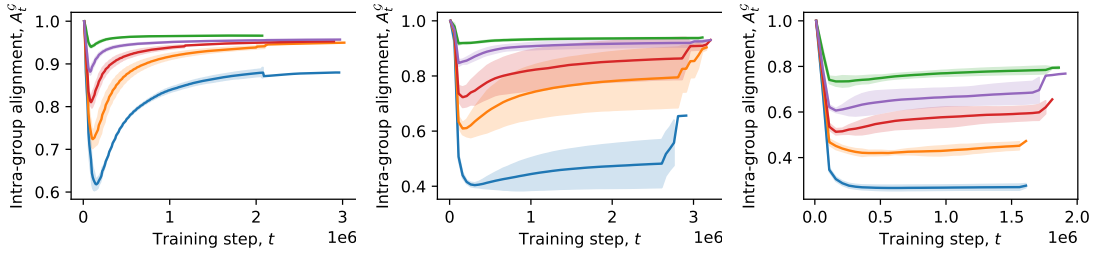


Figure 10: Intra-group alignment A_t^G in the single path task (left), merging paths task (middle) and best-of-ten paths task (right)

during the exploration phase, compared to other tasks, and that the small-world is the slowest to align with all other structures. Perhaps this explains why this topology finds the optimal solution with the least probability: by propagating information quickly, the group early on converges to the local optimum in this task. In the best-of-ten task, the no-sharing setting has the smallest alignment with all other structures. This reinforces our main conclusion in this work: experience sharing affects individuals and different topologies do so in different ways.

7.4.4 Effect of group size

We here examine the effect of the group size for all social network structures in the crossing paths and best-of-ten paths task. To visualize the progression of a group on the paths of the different tasks, we focus on specific elements in the tasks: (i) $[A_8, B_8, C_2]$ in the crossing paths task. The first two correspond to reaching the end of the paths corresponding to the two local optima. To reduce the computational complexity of experiments, we do not study the last element of the optimal path (C_4),

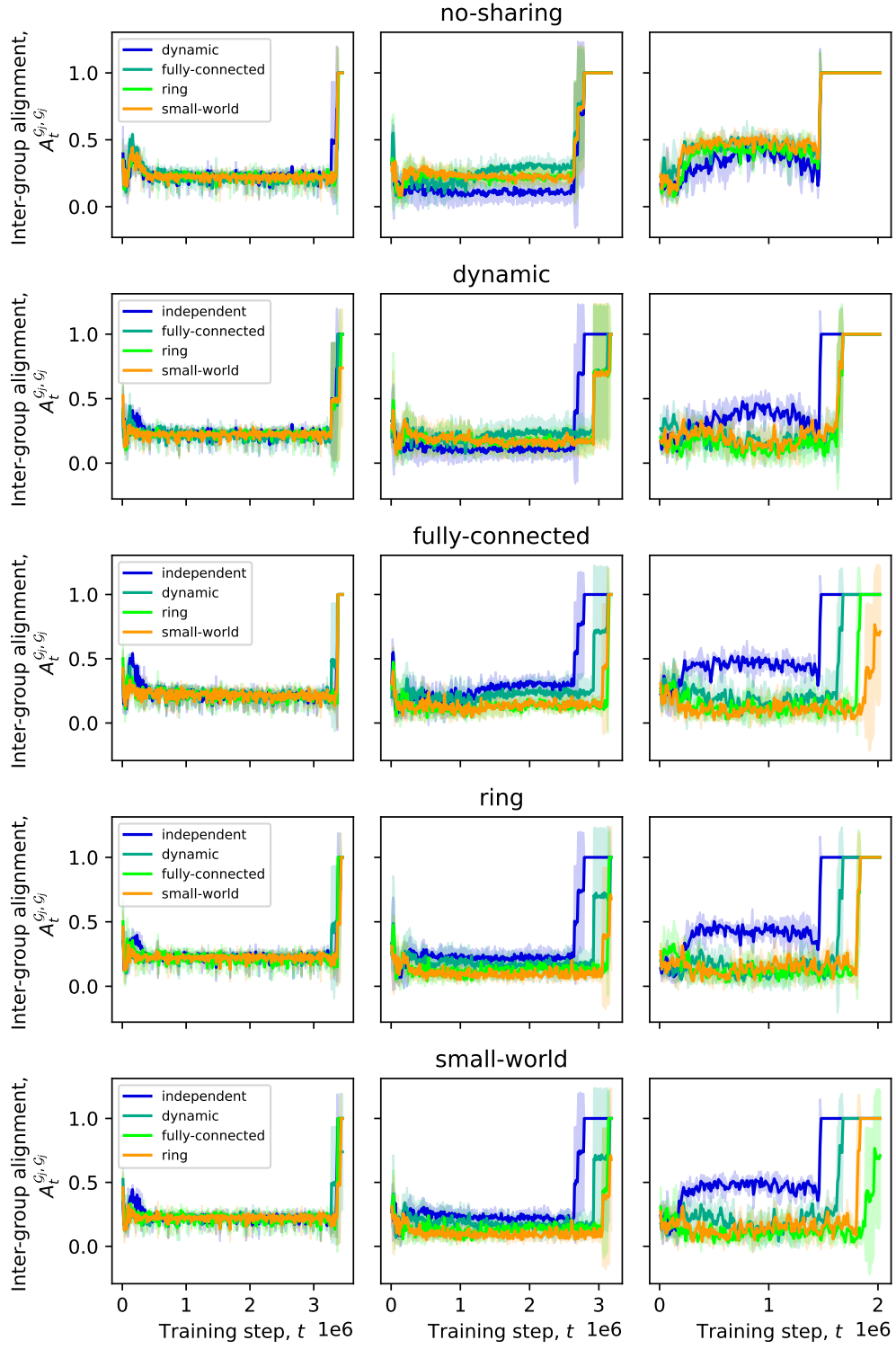


Figure 11: Inter-group alignment $A_t^{G_i, G_j}$ in the single path task (left), merging paths task (middle) and best-of-ten paths task (right). In each row we compare one topology with all the rest.

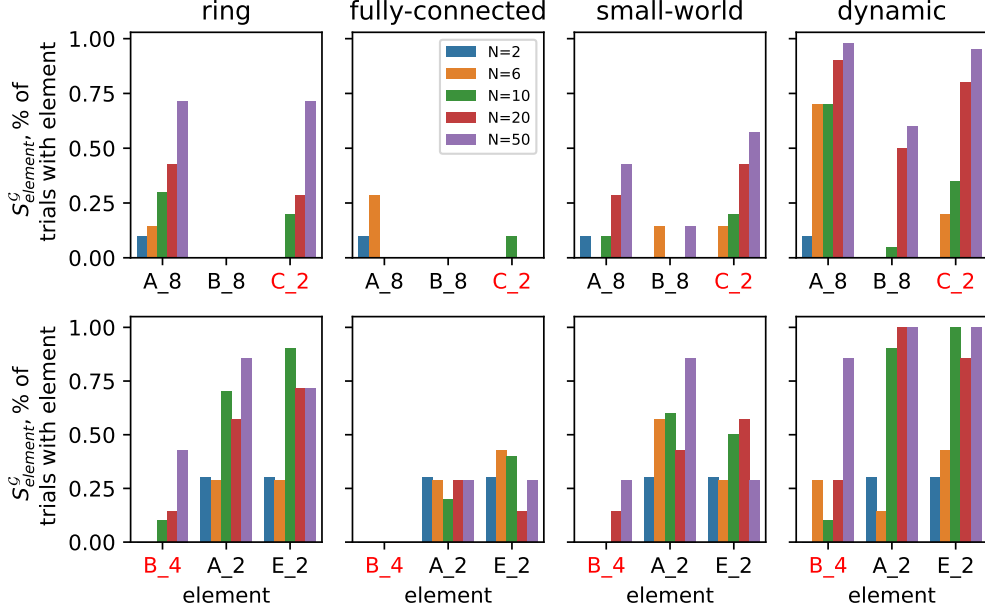


Figure 12: Scaling of different social network structures in the merging paths (top row) and best-of-ten paths tasks (bottom row). We highlight the element belonging to the optimal path in red.

but focus on C_2 instead. This is sufficient to detect whether a group has discovered the optimum path. Here, we observe that the fully-connected topology fails to find the optimal path regardless of its size (with a small success probability for $N = 10$). We observe that the ability of the ring, small-world and dynamic topologies to avoid the local optima improves with the group size (ii) $[B_4, A_2, E_2]$ in the best-of-ten tasks. B_4 is the fourth element on the optimal path (again we do not study the last element to reduce complexity). To avoid cluttering the visualization we only present two of the nine sub-optimal paths. In this task, we again observe that the fully-connected network fails to discover the optimal task. Among all structures and group sizes, the large dynamic network performs best, while the performance of ring and small-world is also best for $N = 50$. We observe that small networks sizes ($N = 2, N = 6$) are slower at exploring (we can see that as they rarely find the second element of the sub-optimal paths, which is required to conclude that path B is the optimal choice).

Overall, **this scaling analysis indicates that increasing the group size in a fully-connected topology will not improve performance, while benefits are expected for low-connectivity structures, particularly for the dynamic topology.** We believe that this observation is crucial. In studies of groups of both human and artificial agents, we often encounter the conviction that, larger groups perform better and that size is a more important determinant than connectivity, the latter justifying why connectivity is often ignored Kline and Boyd (2010); Horgan et al. (2018); Mnih et al. (2016); Schmitt et al. (2019); Nair et al. (2015). Our results here point to the contrary.

7.4.5 Varying dynamic topologies

We now examine the performance of the dynamic-periodic topology for various values of T_h and T_l . **In the merging paths task (left of Figure 13) medium values for the period of both phases works best, while there is some success when the low connectivity phase lasts long ($T_l = 1000$).** **In the best-of-ten paths task (right of Figure 13), we observe the same medium values for the period of both phases work best: thus both the absolute value and their ratio is important to ensure that exploration is efficient. The optimal configuration is the same between the two tasks ($T_l = 100, T_h = 10$), which is a good indication of the robustness of this structure.**

In Figure 14, we observe the % of group success (S^G) with the dynamic-Boyd topology for different probabilities of visit (p_v) and visit duration T_v (the sub-group size is 2 in all cases). We note that, due to our implementation choice that a visit can take place only if no other agent is currently on a visit,

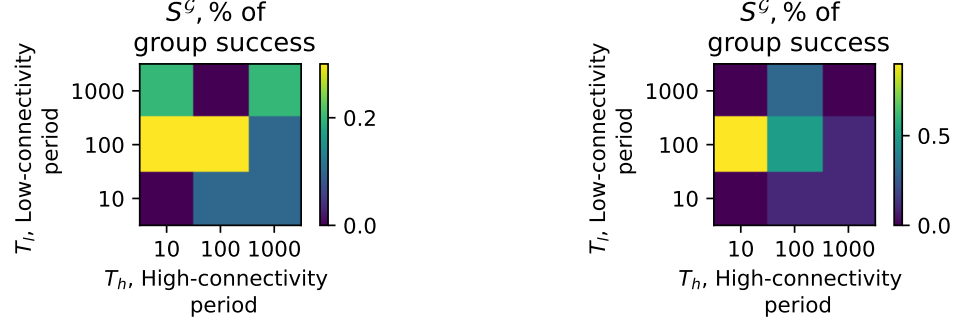


Figure 13: Examining the sensitivity of the dynamic-periodic topology to its hyper-parameters: % of group success (S^G) for the crossing paths task (left) and the best-of-ten paths task (right).

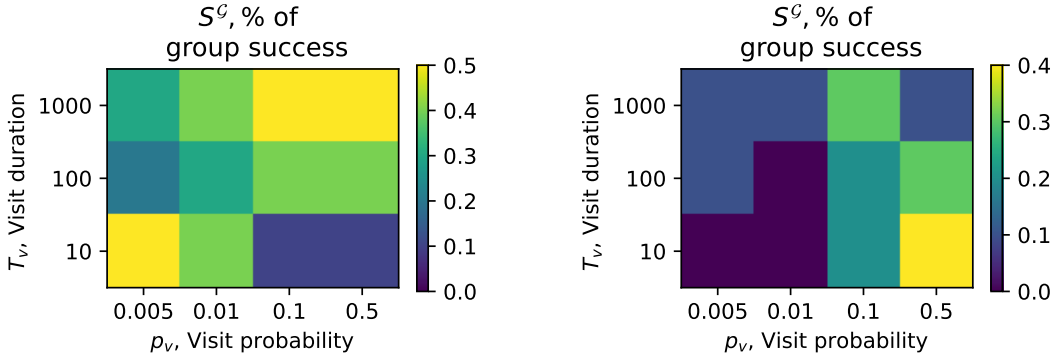


Figure 14: Examining the sensitivity of the dynamic-Boyd topology to its hyper-parameters: % of group success (S^G) for the crossing paths task (left) and the best-of-ten paths task (right).

the visit duration also affects the mixing of the group: longer visits mean that fewer visits will take place in total. **In the merging paths task (left), two hyper-parameter settings have a clear effect: (i) short visits with of high probability lead to bad performance. As such settings lead to a quick mixing of the population, they lead to convergence to the local optimum (ii) long visits with high probability work well. Due to the high visit probability, this setting effectively leads to topology where exactly one agent is always on a long visit. Thus, it ensures that sub-groups stay isolated for at least 1000 episodes, after which inter sub-group sharing needs to takes place to ensure that the sub-groups can progress quickly. In the best-of-ten paths task (right), this structure has a clear optimal hyper-parameterization: short visits with high probability are preferred, which maximizes the mixing of the group and makes early exploration more effective.**